Vietnam Journal of Mechanics, Vol. 48, No. 1 (2026), pp. 23 – 41
DOI: https://doi.org/10.15625/0866-7136/23064

A NEW OPTIMAL CONTROL SCHEME WITH ADJUSTABLE GAIN FEATURED BY SATURATION FUNCTION AND ITS SWITCHING MODELS FOR NON-SMOOTH VIBRATIONS

Xuan Phu Do[1,2]
[1]*Department of Mechatronics and Sensor Systems Technology, Vietnamese-German University, Thoi Hoa, Ho Chi Minh city, Vietnam*
[2]*Department of Mechatronics, Vietnamese-German University, Thoi Hoa, Ho Chi Minh city, Vietnam*
E-mail: phu.dx@vgu.edu.vn

Received: 21 June 2025 / Revised: 21 September 2025 / Accepted: 15 October 2025
Published online: 29 March 2026

Abstract. In this study, a new optimal control scheme with two proposed theorems is presented. Two optimal control theorems are developed: (i) the first scheme uses the conventional adaptive gain with a new proposed saturation function, and (ii) the second scheme utilizes a new adaptive switching saturation function based on the first model (i). In the first model, the derivative result is derived in a new form of exponential function of the saturation function. The adaptive gain for this model includes system states with a chosen matrix of the Hamiltonian equation. In the second model, a new switching saturation is adopted. The constraints related to the system states and the chosen matrix are then applied. Unlike the first control scheme, the second scheme uses the required boundary of the system state for choosing the adaptive gain. The properties of the saturation function used in the first model are still applied in the second model. The main advantage of this second model is to provide flexibility in computing the gain under severe disturbance through the initial boundaries and adjusting the energy consumption of the control system. After the formulation, the proposed controllers with the new adaptive gains are applied to a vehicle seat suspension system with non-smooth vibrations. Two existing controllers are also chosen for this simulation to compare with the proposed models. The simulation results show that the proposed control schemes can provide better control performances in terms of the PSD index (power spectral density), displacement, and control input signal.

Keywords: switching saturation function, switching optimal control, non-smooth vibration, seat suspension system, severe disturbance.

NOMENCLATURE

$x_\nabla(t) \in R^n$	The state vector.
$u_\nabla(t) \in R^l$	The control input.
$B_\nabla(t)$	A time-varying function.
$a_{1\nabla}$	The matrix of size $n \times n$.
$a_{p\nabla}$	The $(p+1)$-dimensional tensor of $n \times ..._{(p+1)times}... \times n$.
$x \times ..._{p\ times}... \times x$	The p-dimensional tensor of $n \times ..._{p\ times}... \times n$ obtained by p-times spatial multiplication of $x_\nabla(t)$.
$R_\nabla(t)$	The positive-definite symmetric matrix function.
$\psi_\nabla, L_\nabla(t)$	Symmetric positive-definite matrices.
α	A positive constant.

$q_{\nabla}(t)$	Defined with the new saturation function as $q_{\nabla}(t) = \alpha Q_{\nabla}(t)\,\text{funsat}[x_{\nabla}(t)]$.
$u_{e\nabla}(t)$	The input control.
ν	A constant.
k_1 and k_2	Constants associated with the setup boundary and the order of the signum function.
δ	The setup boundary.
r	The order of the signum function in the first case.
β	The order of the signum function in the second case.

1. INTRODUCTION

Modern devices require modern controllers to obtain good performances. This statement holds true at any time, especially with the rapid development of new actuators with advanced technologies. Optimal controllers have been frequently used as a priority choice for many dynamic control systems because of their simple structure, robustness of the stability, and easy facilitation in the applications. Hence, many new types of optimal controllers have been continuously developed based on new theories, models, and applications. An adaptive optimal controller, which combines neural networks and the Bellman equation, was presented in Modares et al. (2013). The Bellman equation in Modares et al. (2013) was applied as the policy iteration in the optimization process, which was simplified from the Hamilton-Jacobi-Bellman function. The tanh function was embedded into the Bellman equation to facilitate the calculation. It is remarked that the tanh function is applied in Modares et al. (2013) with its role as the pre-boundary for the Bellman equation. The application of game theory based on the Nash strategy for adaptive optimal control was proposed in Karg et al. (2023). The Nash strategy in Karg et al. (2023) helps to improve the efficiency in choosing the optimized parameters. The policy iteration method in Karg et al. (2023) differs from the iteration in Modares et al. (2013) by defining a new optimal control law based on the gradient descent method. The gradient descent method is a classical approach with the advantage of saving computation time. The Nash model can be seen as the replacement for neural networks as shown in Modares et al. (2013). The barrier function has been used as a policy iteration scheme in Xiao et al. (2022) under the supervision of the Lyapunov function. The optimal controller in Kikuuwe et al. (2022) is similar to the proposed controller in Modares et al. (2013). The same method using neural networks in the optimal controller developed in Modares et al. (2013) and Song et al. (2016) was presented in Vamvoudakis et al. (2016) with the modification of the iteration using Kleiman's algorithm. The gradient descent method can be replaced by the Polak-Ribiere-Polyak conjugate gradient method, as shown in P. Liu et al. (2022). The Hermite-Simpson direct collocation method can be used for designing the iteration method of the optimal control law, as shown in Soler et al. (2016). The methods proposed in (P. Liu et al., 2022; Soler et al., 2016) are good solutions for the optimization process, but their disadvantage is the complex calculation, which reduces the efficiency of the controller. Therefore, the modification based on the conventional model of the Riccati differential equation was proposed in Deng and Shen (2021). In fact, the model in Deng and Shen (2021) is a kind of Hurwitz model with a jump function. The jump function in Deng and Shen (2021) adapts its values according to the system states. As aforementioned, the game theory with the Nash strategy can improve its performance with the multivariate probabilistic collocation method, as shown in M. Liu et al. (2020). The complicated calculation of the Nash strategy can be simplified by using a sliding-mode-like function as in Basin et al. (2012). In this model, the Hamiltonian function was still the main form in the control design, and the sliding-like function was added to reduce the complexity, as shown in Basin et al. (2012). The model developed in Basin et al. (2012) is a good reference, which shows how to incorporate other control forms into the optimal controllers to increase the flexibility and applicability of the new

controllers to real systems. Another form of the Riccati-like equation was studied in Zhang et al. (2018) based on the Hamiltonian function. The adaptive gain function for the optimal control with the sliding-like model was improved in Phu et al. (2020). The gain in Phu et al. (2020) was proposed with the state variable in the form, and the exponential order was not larger than the second order. The gain function in Phu et al. (2020) can also provide a feasible solution for the gains of both the optimal controller and other controllers. The adaptive optimal controller using both the fuzzy model and neural networks for the dead-zone band and time delay was presented in Phu and Mien (2020). Normally, the dead-zone band is defined in a simplified form, which affects the system errors. The dead-zone model was designed in the nonlinear form with two branches of forward and feed-forward types. The unified model of hybrid control combining the dead-zone model and time delay was studied in Phu and Mien (2020). The combination method consisting of the conventional optimal control, H-infinity technique, the classical sliding mode control, and prescribed performance has been developed for systems with severe disturbances in Phu Do et al. (2019). Another choice of neural network and prescribed sliding surface can be used with the optimal control law as in Phu et al. (2018).

From the above literature analysis, the optimal control method has been proven to be a good candidate for handling external disturbances and severe uncertainties for many challenging control systems such as smart material-based vehicle suspension systems. However, there are still many opportunities for improving its efficiency, especially when it is integrated with other controllers. In this study, two new optimal controllers are developed based on two newly suggested saturation functions. Consequently, the main technical contributions of this study can be highlighted as follows: (1) A new modified saturation function is proposed for the formulation of a new optimal control system. This model overcomes the disadvantages of the conventional saturation function, which cannot use the derivative form of the saturation function when designing the controller. (2) A new adaptive gain equation is proposed for the new modified saturation function when designing the optimal control scheme. (3) A new switching saturation-like gain function is proposed in combination with an exponential function and a signum function. This controller possesses an outstanding property in terms of computational flexibility. In addition, a new adaptive switching saturation-like gain equation is derived for the optimal controller. (4) Simulations are carried out to validate the superior control performances of the proposed optimal schemes over the traditional optimal controller by applying the controllers to a vehicle seat damper system.

The rest of this paper is organized as follows: Section 2 presents the design of new optimal control laws, Section 3 shows the simulation results of the proposed controllers compared with two existing controllers, and Section 4 provides the conclusions with a summary of the main findings of the proposed control in both development and simulation results.

2. DESIGN OF NEW OPTIMAL CONTROL LAWS

2.1. Proposed model 1: Adaptive gain with new saturation function

The proposed control is designed following a linear-like equation given by

$$\dot{x}_{\nabla}(t) = f_{\nabla}(x_{\nabla}, t) + B_{\nabla}(t)\, u_{\nabla}(t), \tag{1}$$

where $x_{\nabla}(t) \in R^n$ is the state vector, $u_{\nabla}(t) \in R^l$ is the control input vector, and $B_{\nabla}(t)$ is a time-varying function. The function $f_{\nabla}(x_{\nabla}, t)$ is defined as follows

$$f_{\nabla}(x_{\nabla}, t) = a_{0\nabla}(t) + a_{1\nabla}(t)\, x_{\nabla}(t) + a_{2\nabla}(t)\, x_{\nabla}(t)\, x_{\nabla}^{T} + \ldots + a_{p\nabla}(t)\, x_{\nabla}(t) \ldots_{p\ times} \ldots x_{\nabla}(t),$$

where $a_{0\nabla}$ is the vector of dimension n, $a_{1\nabla}$ is the matrix of size $n \times n$, $a_{p\nabla}$ is the $(p+1)$-dimensional tensor of size $n \times \ldots_{(p+1)times} \ldots \times n$, and $x \times \ldots_{p\ times} \ldots \times x$ is the p-dimensional tensor of size $n \times \ldots_{p\ times} \ldots \times n$ obtained by p-times spatial multiplication of $x_{\nabla}(t)$. The cost

function of the first proposed control is applied as follows

$$J_1 = \sum_{i=1}^{n} \frac{\psi_{\nabla ii} \left| x_{\nabla i} \left(T \right) \right|}{\alpha} + \frac{1}{2} \int_{t_0}^{T} \left(u_{\nabla}^{T} \left(s \right) R_{\nabla} \left(s \right) u_{\nabla} \left(s \right) + x_{\nabla}^{T} \left(s \right) L_{\nabla} \left(s \right) x_{\nabla} \left(s \right) \right) \mathrm{d}s, \tag{2}$$

where $R_{\nabla}\left(t\right)$ is the positive-definite symmetric matrix function; $\psi_{\nabla}, L_{\nabla}\left(t\right)$ are symmetric-positive-definite matrices; $\psi_{\nabla} \geq 0, L_{\nabla}\left(t\right) \geq 0$, and α is a positive constant. The optimal control law is described as follows

$$u_{\nabla}^{*}\left(t\right) = -R_{\nabla}^{-1}\left(t\right) {B_{\nabla}}^{T}\left(t\right) q_{\nabla}\left(t\right), \tag{3}$$

where $q_{\nabla}\left(t\right)$ is the gain function which is defined with the new saturation function as

$$q_{\nabla}\left(t\right) = \alpha Q_{\nabla}\left(t\right) \mathrm{funsat}\left[x_{\nabla}\left(t\right)\right], \tag{4}$$

where $x_{\nabla} = \left[x_{1\nabla}, \ldots, x_{n\nabla}\right] \in R^n$, $\mathrm{funsat}\left[x_{\nabla}\left(t\right)\right] = \left[\mathrm{funsat}\left(x_{1\nabla}\right), \ldots, \mathrm{funsat}\left(x_{n\nabla}\right)\right] \in R^n$, and $Q_{\nabla}\left(t\right)$ is the symmetric gain matrix of size $n \times n$. The 'funsat' function is proposed as follows

$$\mathrm{funsat}\left[x_{\nabla}\left(t\right)\right] = \frac{2}{1 + e^{-2x_{\nabla}(t)}} - 1. \tag{5}$$

The properties of the funsat function include $\left| \frac{\mathrm{d}\left(\mathrm{funsat}\left[x_{\nabla}\left(t\right)\right]\right)}{\mathrm{d}t} \right| \leq 1$, $\mathrm{funsat}'\left[0\right] = 1$, and $\left|\mathrm{funsat}\left[x_{\nabla}\left(t\right)\right]\right| \leq 1$.

From Eq. (4), Eq. (3) is rewritten as follows

$$u_{\nabla}^{*}\left(t\right) = -R_{\nabla}^{-1}\left(t\right) {B_{\nabla}}^{T}\left(t\right) \left(\alpha Q_{\nabla}\left(t\right) \mathrm{funsat}\left[x_{\nabla}\left(t\right)\right]\right). \tag{6}$$

Using Eq. (6), the system (1) can be written as follows

$$\dot{x}_{\nabla}\left(t\right) = f_{\nabla}\left(x, t\right) - B_{\nabla}\left(t\right) R_{\nabla}^{-1}\left(t\right) {B_{\nabla}}^{T}\left(t\right) \left(\alpha Q_{\nabla}\left(t\right) \mathrm{funsat}\left[x_{\nabla}\left(t\right)\right]\right). \tag{7}$$

The value $Q_{\nabla}\left(t\right)$ is obtained based on the result of the first derivative equation as follows

$$\dot{Q}_{\nabla}\left(t\right) = L_{\nabla} {x_{\nabla}(t)}^{2} - \alpha x_{\nabla}\left(t\right) Q_{\nabla}\left(t\right). \tag{8}$$

The derivation of $Q_{\nabla}\left(t\right)$ is shown in Appendix A. By solving Eq. (8), a new optimal value $Q_{\nabla}^{*}\left(t\right)$ can be found and then substituted into Eq. (6) as follows

$$u_{\nabla}^{*}\left(t\right) = -R_{\nabla}^{-1}\left(t\right) {B_{\nabla}}^{T}\left(t\right) Q_{\nabla}^{*}\left(t\right). \tag{9}$$

Hence, Eq. (7) can be rewritten as follows

$$\dot{x}_{\nabla}\left(t\right) = f_{\nabla}\left(x, t\right) - B_{\nabla}\left(t\right) R_{\nabla}^{-1}\left(t\right) {B_{\nabla}}^{T}\left(t\right) Q_{\nabla}^{*}\left(t\right). \tag{10}$$

Remark 2.1. *The newly proposed saturation function (5) can be differentiated with respect to time. This property does not exist in the conventional saturation form. The adaptive gain function (8) is solved with respect to the second order of the system state $x_{\nabla}\left(t\right)$ to obtain the target optimized gain value for the control input. The differences between the proposed models (5, 8) and the model in Phu et al. (2020) will be pointed out and compared in the simulation section.*

Remark 2.2. *The optimal controls (Basin et al., 2011, 2012) were developed based on the conventional signum function in the input control function. These models (Basin et al., 2011, 2012) could not be applied to a system in the presence of severe disturbances. However, the proposed optimal control (6) with the application of the newly proposed saturation function (5) can overcome the disadvantage of the conventional signum function. In addition, the control (Basin et al., 2012) had been chosen to compare with the research in (Phu et al., 2020). Hence, the choice of (Phu et al., 2020) in comparison with the proposed model expressed in Theorem 1 is a good choice for evaluating the properties instead of using the method in (Basin et al., 2011, 2012).*

Theorem 2.1. *The control system (1) with the cost function (3) is integrated with the control law (9) and the derivative of the gain matrix function (8). Then, the optimal control state of the linear system (1) is re-written by the system (10).*

Proof. The candidate Hamiltonian function for the optimal control is established as

$$H\left(x_{\nabla}, u_{\nabla}, q_{\nabla}, t\right) = \frac{1}{2}\left(u_{\nabla}^{T} R_{\nabla}\left(t\right) u_{\nabla} + x_{\nabla}^{T} L_{\nabla}\left(t\right) x_{\nabla}\right) + q_{\nabla}^{T} \dot{x}_{\nabla}\left(t\right). \tag{11}$$

The optimal control law u_{∇} is then obtained by using the maximum principle $\frac{\partial H}{\partial u_{\nabla}} = 0$ as follows

$$u_{\nabla}^{*}\left(t\right) = -R_{\nabla}^{-1}\left(t\right) B_{\nabla}^{T}\left(t\right) q_{\nabla}\left(t\right). \tag{12}$$

Now, substituting Eq. (4) into Eq. (12) yields the following main control input

$$u_{\nabla}^{*}\left(t\right) = R_{\nabla}^{-1}\left(t\right) B_{\nabla}^{T}\left(t\right)\left(\alpha Q_{\nabla}\left(t\right) \text{funsat}\left[x_{\nabla}\left(t\right)\right]\right). \tag{13}$$

Applying the co-state equation given by $\frac{\mathrm{d}q_{\nabla}\left(t\right)}{\mathrm{d}t} = -\frac{\partial H}{\partial x_{\nabla}}$, the following equation is obtained.

$$-\frac{\mathrm{d}q_{\nabla}\left(t\right)}{\mathrm{d}t} = L_{\nabla}\left(t\right) x_{\nabla}\left(t\right) + \left[\frac{\partial f_{\nabla}\left(x_{\nabla}, t\right)}{\partial x_{\nabla}}\right]^{T} q_{\nabla}\left(t\right). \tag{14}$$

From Eq. (5) and the definition of $f_{\nabla}\left(x, t\right)$, Eq. (14) can be rewritten as follows

$$\begin{aligned} &-\alpha \dot{Q}_{\nabla}\left(t\right) \text{funsat}\left[x_{\nabla}\left(t\right)\right] - \alpha Q_{\nabla}\left(t\right) \frac{\mathrm{d}\left(\text{funsat}\left[x_{\nabla}\left(t\right)\right]\right)}{\mathrm{d}t} \\ &= L_{\nabla}\left(t\right) x\left(t\right) + \alpha\left[\frac{\partial f_{\nabla}\left(x, t\right)}{\partial x_{\nabla}}\right]^{T} Q_{\nabla}\left(t\right) \text{funsat}\left[x_{\nabla}\left(t\right)\right]. \end{aligned} \tag{15}$$

Now, the derivative of $f_{\nabla}\left(x, t\right)$ is obtained by

$$\frac{\partial f_{\nabla}\left(x, t\right)}{\partial x_{\nabla}} = a_{1\nabla} + 2a_{2\nabla} x_{\nabla} + 3a_{3\nabla} x_{\nabla} x_{\nabla}^{T} + ... + p a_{p\nabla} x_{\nabla} ... {}_{(p-1)times} ... x_{\nabla}. \tag{16}$$

Using Eqs. (15) and (16), the following equation is obtained

$$\begin{aligned} &-\alpha \dot{Q}_{\nabla}\left(t\right) \text{funsat}\left[x_{\nabla}\left(t\right)\right] - \alpha Q_{\nabla}\left(t\right) \frac{\mathrm{d}\left(\text{funsat}\left[x_{\nabla}\left(t\right)\right]\right)}{\mathrm{d}t} = L_{\nabla}\left(t\right) x_{\nabla}\left(t\right) \\ &+ \alpha\begin{bmatrix} a_{1\nabla} + 2a_{2\nabla} x_{\nabla} + 3a_{3\nabla} x_{\nabla} x_{\nabla}^{T} + ... \\ + p a_{p\nabla} x_{\nabla} ... {}_{(p-1)times} ... x_{\nabla} \end{bmatrix}^{T} Q_{\nabla}\left(t\right) \text{funsat}\left[x_{\nabla}\left(t\right)\right]. \end{aligned} \tag{17}$$

Using the property of $\left|\frac{\mathrm{d}\left(\text{funsat}\left[x_{\nabla}\left(t\right)\right]\right)}{\mathrm{d}t}\right| \leq 1$, Eq. (17) is re-expressed as follows

$$\begin{aligned} &\alpha \dot{Q}_{\nabla}\left(t\right) \text{funsat}\left[x_{\nabla}\left(t\right)\right] = -L_{\nabla}\left(t\right) x_{\nabla}\left(t\right) \\ &- \alpha\begin{bmatrix} a_{1\nabla} + 2a_{2\nabla} x + 3a_{3\nabla} x_{\nabla} x_{\nabla}^{T} + ... \\ + p a_{p\nabla} x_{\nabla} ... {}_{(p-1)times} ... x_{\nabla} \end{bmatrix}^{T} Q_{\nabla}\left(t\right) \text{funsat}\left[x_{\nabla}\left(t\right)\right] - \alpha Q_{\nabla}\left(t\right). \end{aligned} \tag{18}$$

Thus, if $x_{\nabla}\left(t\right) = 0$, then $u_{\nabla}\left(t\right) = 0$. The value of $Q_{\nabla}\left(t\right)$ is not required. If $Q_{\nabla}\left(t\right)$ is the solution of Eq. (8), then, the result of Eq. (10) is satisfied. On the other hand, Eq. (4) can be written at time $t = T$ as follows

$$q_{\nabla}\left(T\right) = \alpha Q_{\nabla}\left(T\right) \text{funsat}\left[x_{\nabla}\left(T\right)\right]. = \frac{\partial J}{\partial x_{\nabla}\left(T\right)} = \frac{\psi_{\nabla}}{\alpha} \text{funsat}\left[x_{\nabla}\left(T\right)\right]. \tag{19}$$

Hence, the value $Q_\nabla(T)$ is found from the following equation.

$$Q_\nabla(T) = \frac{\psi_\nabla}{\alpha^2}. \tag{20}$$

Now, the proof of Theorem 2.1 is completed. The flowchart of the proposed controller stated in Theorem 2.1 is shown in Fig. 1. □

Remark 2.3. *The result (20) shows that the result of the gain function is always positive. This result is similar to the result in Phu et al. (2020).*

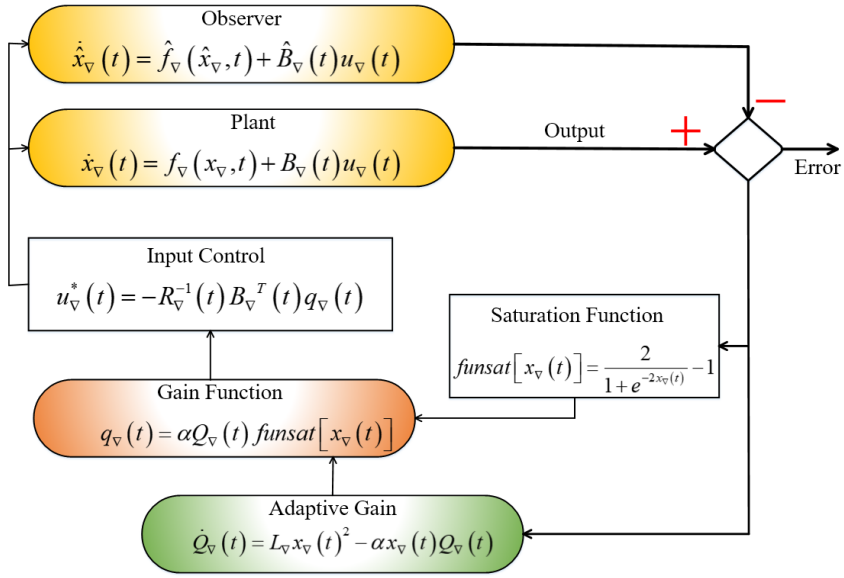

Fig. 1. The computational flowchart of the first proposed controller scheme

2.2. Proposed model 2: Adaptive switching saturation-like gain function

In this design, the proposed gain function is described as follows

$$q_{e\nabla}(t) = \begin{cases} \alpha_e Q_{e\nabla}\left(k_1 sig^r(x_{e\nabla}) + k_2 \delta^{|x_{e\nabla}|} x_{e\nabla}\right) & \text{if } |x_{e\nabla}| < \delta, \\ \alpha_e Q_{e\nabla} sig^\beta(x_{e\nabla}) & \text{if } |x_{e\nabla}| > \delta, \end{cases} \tag{21}$$

where $k_1 = \dfrac{-1 - \ln\delta}{\beta - \delta\ln\delta}$ and $k_2 = \dfrac{\delta^{2\beta-2}}{\beta - \delta\ln\delta}$ are constants associated with the setup boundary and the order of the signum function, $\delta \in \left(0, e^{-1}\right)$ is the setup boundary, $r = 2 - \delta$ is the order of the signum function in the first case, $\beta = 1 - \delta$ is the order of the signum function in the second case.

Remark 2.4. *The function $sig^r(x_{e\nabla})$ is defined as follows (Sai et al., 2022)*

$$sig^r(x_{e\nabla}) = |x_{e\nabla}|^r sign(x_{e\nabla}), r > 0. \tag{22}$$

Remark 2.5. *The relation between the saturation and signum functions can be expressed as follows*

$$sat(x_{e\nabla}) = \begin{cases} sign(x_{e\nabla}) & if\ |x_{e\nabla}| \geq x_{\max} \\ x_{e\nabla} & if\ |x_{e\nabla}| < x_{\max} \end{cases}. \tag{23}$$

Hence, the defined function (22) is a part of the saturation function, as shown in (23). The input control $u_{e\nabla}(t)$ is determined as follows

$$u^*_{e\nabla}(t) = \begin{cases} -\alpha_e R^{-1}_{e\nabla} {B_{e\nabla}}^T Q_{e\nabla} \left(k_1 sig^r(x_{e\nabla}) + k_2 \delta^{|x_{e\nabla}|} x_{e\nabla} \right) & \text{if } |x_{e\nabla}| < \delta, \\ -\alpha_e R^{-1}_{e\nabla} {B_{e\nabla}}^T Q_{e\nabla} sig^\beta(x_{e\nabla}) & \text{if } |x_{e\nabla}| > \delta, \end{cases} \tag{24}$$

where, the optimized gain function $Q_{e\nabla}$ is found as follows

$$\dot{Q}_{e\nabla} = \begin{cases} -\alpha_e L_{e\nabla} x^2_{e\nabla} - \nu \left(a_{1e\nabla} - \alpha_e k_1 r x^2_{e\nabla} \right) Q_{e\nabla} & \text{if } |x_{e\nabla}| < \delta, \\ -\alpha_e L_{e\nabla} x^2_{e\nabla} - \nu \left(a_{1e\nabla} - \alpha_e \beta x^2_{e\nabla} \right) Q_{e\nabla} & \text{if } |x_{e\nabla}| > \delta, \end{cases} \tag{25}$$

where, ν is a constant. The proof of Eq. (25) is shown in Appendix B. In this case, the cost function is defined based on (2) as follows (Phu et al., 2020)

$$J_2 = \sum_{i=1}^{n} \frac{\psi_{\nabla ii} |x_{e\nabla}(T)|}{\alpha_e} + \frac{1}{2} \int_{to}^{T} \left(u^T_{e\nabla}(s) R_{e\nabla}(s) u_{e\nabla}(s) + x^T_{e\nabla}(s) L_{e\nabla}(s) x_{e\nabla}(s) \right) \mathrm{d}s. \tag{26}$$

Remark 2.6. *The adaptive gain function (25) is a new contribution to developing the adaptive gain for the optimal controllers, which preserves the main properties of the system. This modification is the main difference compared with the gain function (8) and represents the key novelty of this investigation. This result will help to reduce the control energy when controlling a system.*

Theorem 2.2. *The control system (1) with the cost function (26) is integrated with the control law (24) and the adaptive gain matrix function (25). Then, the optimal control state of the linear system (1) is re-written as*

$$\dot{x}_{e\nabla}(t) = f_{e\nabla}(x_{e\nabla}, t) - \left(\alpha_e R^{-1}_{e\nabla}(t) {B_{e\nabla}}^T(t) Q_{e\nabla} \left\{ \begin{matrix} \left(k_1 sig^r(x_{e\nabla}) + k_2 \delta^{|x_{e\nabla}|} x_{e\nabla} \right) & if\ |x_{e\nabla}| < \delta \\ sig^\beta(x_{e\nabla}) & if\ |x_{e\nabla}| > \delta \end{matrix} \right\} \right). \tag{27}$$

Proof. The candidate of Hamiltonian function of optimal control is established by

$$H(x_{e\nabla}, u_{e\nabla}, q_{e\nabla}, t) = \frac{1}{2} \left(u^T_{e\nabla} R_{e\nabla}(t) u_{e\nabla} + x^T_{e\nabla} L_{e\nabla}(t) x_{e\nabla} \right) + q^T_{e\nabla} \dot{x}_{e\nabla}(t). \tag{28}$$

The optimal control law $u_{e\nabla}$ is then found by using maximum principle $\frac{\partial H}{\partial u_{e\nabla}} = 0$ as follows

$$u^*_{e\nabla}(t) = -R^{-1}_{e\nabla}(t) {B_{e\nabla}}^T(t) q_{e\nabla}(t). \tag{29}$$

This result is identified as Eq. (24). Applying the co-state equation given by $\frac{\mathrm{d}q_{e\nabla}(t)}{\mathrm{d}t} = -\frac{\partial H}{\partial x_{e\nabla}}$, the following equation is obtained.

$$-\frac{\mathrm{d}q_{e\nabla}(t)}{\mathrm{d}t} = L_{e\nabla}(t) x_{e\nabla}(t) + \left[\frac{\partial f_{e\nabla}(x_{e\nabla}, t)}{\partial x_{e\nabla}} \right]^T q_{e\nabla}(t). \tag{30}$$

Using Eq. (16), the derivative of $f_{e\nabla}(x_{e\nabla}, t)$ is written according to the state variable $x_{e\nabla}(t)$ as

$$\frac{\partial f_{e\nabla}(x_{e\nabla}, t)}{\partial x_{e\nabla}} = a_{1e\nabla} + 2a_{2e\nabla} x_{e\nabla} + 3a_{3e\nabla} x_{e\nabla} x^T_{e\nabla} + ... + p a_{pe\nabla} x_{e\nabla} ...^{(p-1)times} ... x_{e\nabla}. \tag{31}$$

Case 1. $|x_{e\nabla}| < \delta$

Using Eqs. (21), (30), (31), the following equation is obtained

$$\begin{aligned}
&-\alpha_e\dot{Q}_{e\nabla}\left(k_1 sig^r\left(x_{e\nabla}\right)+k_2\delta^{|x_{e\nabla}|}x_{e\nabla}\right)-\alpha Q_{e\nabla}\frac{\mathrm{d}\left(k_1 sig^r\left(x_{e\nabla}\right)+k_2\delta^{|x_{e\nabla}|}x_{e\nabla}\right)}{\mathrm{d}t}\\
&=L_{e\nabla}x_{e\nabla}+\alpha_e\begin{bmatrix}a_{1e\nabla}+2a_{2e\nabla}x_{e\nabla}+3a_{3e\nabla}x_{e\nabla}x_{e\nabla}^T+...+\\+pa_{pe\nabla}x_{e\nabla}\cdots_{(p-1)times}\cdots x_{e\nabla}\end{bmatrix}^T Q_{e\nabla}\left(k_1 sig^r\left(x_{e\nabla}\right)+k_2\delta^{|x_{e\nabla}|}x_{e\nabla}\right).
\end{aligned}\tag{32}$$

The result of (32) can be expanded as

$$\begin{aligned}
&-\alpha_e\dot{Q}_{e\nabla}\left(k_1 sig^r\left(x_{e\nabla}\right)+k_2\delta^{|x_{e\nabla}|}x_{e\nabla}\right)-\alpha Q_{e\nabla}\left(k_1 r|x_{e\nabla}|^{r-1}+k_2\left(|x_{e\nabla}|\ln\delta+1\right)\delta^{|x_{e\nabla}|}\right)\\
&=L_{e\nabla}x_{e\nabla}+\alpha_e\begin{bmatrix}a_{1e\nabla}+2a_{2e\nabla}x_{e\nabla}+3a_{3e\nabla}x_{e\nabla}x_{e\nabla}^T+...+\\+pa_{pe\nabla}x_{e\nabla}\cdots_{(p-1)times}\cdots x_{e\nabla}\end{bmatrix}^T Q_{e\nabla}\left(k_1 sig^r\left(x_{e\nabla}\right)+k_2\delta^{|x_{e\nabla}|}x_{e\nabla}\right).
\end{aligned}\tag{33}$$

Thus, if $x_{e\nabla}(t)=0$, then $u_{e\nabla}(t)=0$. And, the value of $Q_{e\nabla}(t)$ is not required. If $Q_{e\nabla}(t)$is the solution of Eq. (33), then, the result of Eq. (25) is satisfied. On the other hand, Eq. (21) is written at time $t=T$ as follows

$$q_{e\nabla}(T)=\alpha_e Q_{e\nabla}\left(k_1 sig^r\left(x_{e\nabla}\right)+k_2\delta^{|x_{e\nabla}|}x_{e\nabla}\right)=\frac{\partial J_2}{\partial x_{e\nabla}(T)}=\frac{\psi_\nabla}{\alpha_e}sat\left[x_{e\nabla}(T)\right].\tag{34}$$

Hence, the boundary value $Q_{e\nabla}(T)$ is found from the following equation

$$Q_{e\nabla}(T)\le\frac{\psi_{e\nabla}}{\alpha_e^2}.\tag{35}$$

Case 2. $|x_{e\nabla}|>\delta$

Using Eqs. (21), (30), (31), the following equation is obtained

$$\begin{aligned}
&-\alpha_e\dot{Q}_{e\nabla}sig^\beta\left(x_{e\nabla}\right)-\alpha Q_{e\nabla}\frac{\mathrm{d}\left(sig^\beta\left(x_{e\nabla}\right)\right)}{\mathrm{d}t}\\
&=L_{e\nabla}x_{e\nabla}+\alpha_e\begin{bmatrix}a_{1e\nabla}+2a_{2e\nabla}x_{e\nabla}+3a_{3e\nabla}x_{e\nabla}x_{e\nabla}^T+...\\+pa_{pe\nabla}x_{e\nabla}\cdots_{(p-1)times}\cdots x_{e\nabla}\end{bmatrix}^T Q_{e\nabla}sig^\beta\left(x_{e\nabla}\right).
\end{aligned}\tag{36}$$

The equivalent result (36) can be rewritten by

$$\begin{aligned}
&-\alpha_e\dot{Q}_{e\nabla}sig^\beta\left(x_{e\nabla}\right)-\alpha\beta Q_{e\nabla}|x_{e\nabla}|^{\beta-1}\\
&=L_{e\nabla}x_{e\nabla}+\alpha_e\begin{bmatrix}a_{1e\nabla}+2a_{2e\nabla}x_{e\nabla}+3a_{3e\nabla}x_{e\nabla}x_{e\nabla}^T+...\\+pa_{pe\nabla}x_{e\nabla}\cdots_{(p-1)times}\cdots x_{e\nabla}\end{bmatrix}^T Q_{e\nabla}sig^\beta\left(x_{e\nabla}\right).
\end{aligned}\tag{37}$$

Thus, if $x_{e\nabla}(t)=0$, then $u_{e\nabla}(t)=0$. And, the value of $Q_{e\nabla}(t)$ is not required. If $Q_{e\nabla}(t)$ is the solution of Eq. (33), then, the result of Eq. (25) is satisfied. On the other hand, Eq. (21) is written at time $t=T$ as follows

$$q_{e\nabla}(T)=\alpha_e Q_{e\nabla}sig^\beta\left(x_{e\nabla}\right)=\frac{\partial J_2}{\partial x_{e\nabla}(T)}=\frac{\psi_\nabla}{\alpha_e}sig\left[x_{e\nabla}(T)\right].\tag{38}$$

Hence, the boundary value $Q_{e\nabla}(T)$ is found from the following equation.

$$Q_{e\nabla}(T)\le\frac{\psi_{e\nabla}}{\alpha_e^2}.\tag{39}$$

Now, the proof of Theorem 2.2 is completed. The computational procedure of Theorem 2.2 is summarized in Fig. 2. □

Remark 2.7. *The composite controls (Li, Liu, & Tong, 2022; Li, Wang, et al., 2022; Sui et al., 2016; Tong et al., 2018) are the combinations of the optimal control with the fuzzy logic control (Sui et al., 2016; Tong et al., 2018) or the neural networks (Li, Liu, & Tong, 2022; Li, Wang, et al., 2022).*

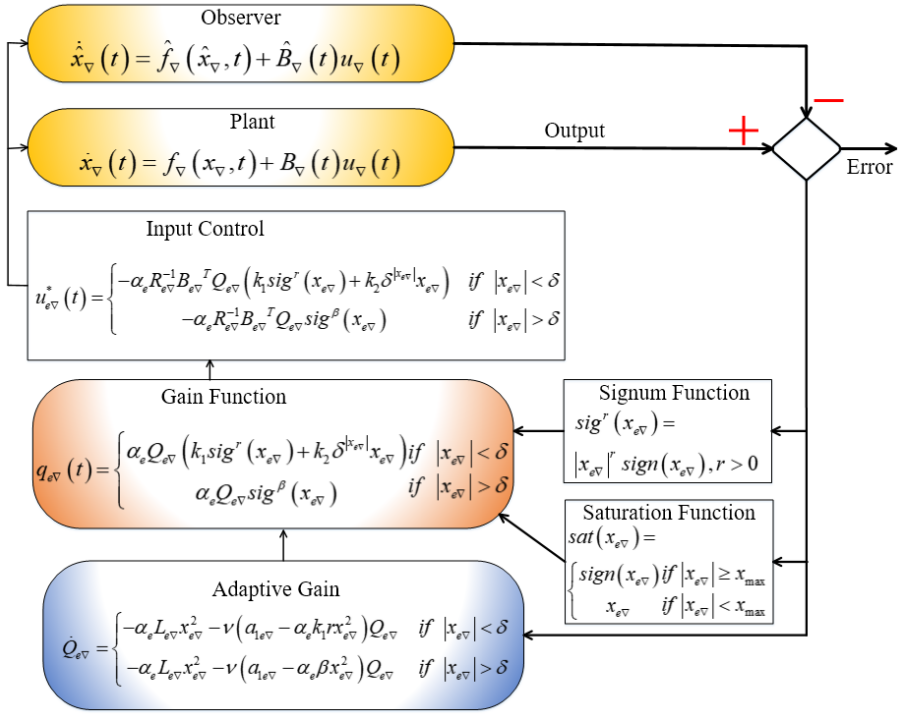

Fig. 2. The computational flowchart of the second proposed controller scheme

3. SIMULATION EXAMPLE AND DISCUSSIONS

In this section, a simulation study is carried out to demonstrate the properties of the proposed controllers. In addition, the proposed controllers are compared with two other state-of-the-art controllers to demonstrate the outstanding performance of the proposed controllers. It is noteworthy that the proposed control can be applied to any system to evaluate its performance. Hence, a complex model of a vehicle seat suspension system treated in Phu and Mien (2020) is used for evaluating the performance of the proposed controllers. The vehicle seat damper is operated with magnetorheological (MR) fluid instead of conventional viscous oil. This system belongs to the semi-active category, which can be controlled by applying the controller according to the variation of the vibration amplitude. The dynamic model of the seat suspension with an MR damper was adopted from the same model used in Phu and Mien (2020), and the proposed controller 1 (Theorem 2.1), the proposed controller 2 (Theorem 2.2), the compared controller 1 in Phu and Mien (2020), and the compared controller 2 in Kikuuwe et al. (2022) are simulated. The governing equations of the system are derived as follows

$$m_s \ddot{x}_s = -k_s (x_s - x_0) - c_s (\dot{x}_s - \dot{x}_0) + k_1 (x_1 - x_s) + c_1 (\dot{x}_1 - \dot{x}_s) + F_{MR}, \tag{40}$$

$$m_1 \ddot{x}_1 = -k_1 (x_1 - x_s) + c_1 (\dot{x}_1 - \dot{x}_s), \tag{41}$$

The above equations are then rewritten using the state variables as follows.

$$\begin{aligned} \dot{x}_{11} &= \dot{x}_s = x_{22}, \quad \dot{x}_{22} = f_{11}(x_{11}, x_{22}, x_{33}, x_{44}) + g_{11}(x_{11}, x_{22}, x_{33}, x_{44}) u, \\ \dot{x}_{33} &= \dot{x}_1 = x_{44}, \quad \dot{x}_{44} = f_{22}(x_{11}, x_{22}, x_{33}, x_{44}), \end{aligned} \tag{42}$$

where,

$$f_{11}\left(x_{11},x_{22},x_{33},x_{44}\right)=-\frac{k_s}{m_s}\left(x_{11}-x_0\right)-\frac{c_s}{m_s}\left(x_{22}-\dot{x}_0\right)+\frac{k_1}{m_s}\left(x_{33}-x_{11}\right)+\frac{c_1}{m_s}\left(x_{44}-x_{22}\right),$$

$$g_{11}\left(x_{11},x_{22},x_{33},x_{44}\right)=\frac{1}{m_s},u=F_{MR},f_{22}\left(x_{11},x_{22},x_{33},x_{44}\right)=-\frac{k_1}{m_1}\left(x_{33}-x_{11}\right)-\frac{c_1}{m_1}\left(x_{44}-x_{22}\right).$$

It is noted that $x_{11},x_{22},x_{33},x_{44}$ are variables according to x_s and x_1 of the system. The calculated result of $u=F_{MR}$ must be converted into the input signal to generate the required magnetic field for MR damper. It is noted that the damping force of the MR damper is established from the piston – rod of the damper when supporting the electric energy into the model. This work is done by applying the relationship given as follows

$$F_{MR}=\left(c_a+c_b\vartheta\right)\left(x_{44}-x_{22}\right)+k_0\left(x_{33}-x_{11}\right)+\left(\alpha_a+\alpha_b\vartheta\right)\phi, \tag{43}$$

where $\dot{\phi}=-\kappa\left|x_{44}-x_{22}\right|+\lambda_d\left(x_{44}-x_{22}\right)\left|\phi\right|+\varphi_d\left(x_{44}-x_{22}\right)$. Using Eq. (36), the voltage of ϑ to be applied to MR damper is found as follows

$$\vartheta=\frac{F_{MR}-\left[c_a\left(x_{44}-x_{22}\right)+k_0\left(x_{33}-x_{11}\right)+\alpha_a\phi\right]}{c_b\left(x_{44}-x_{22}\right)+\alpha_b\phi}. \tag{44}$$

It is noted that the voltage ϑ will be converted into the input current related to the damping force of the MR damper in real applications. The selected parameters of the suspension system are listed in Tables 1–3.

Table 1. Parameters of the seat suspension system (Phu et al., 2020)

Parameter	Value
Mass of seat m_s	27 kg
Mass of driver m_1	77 kg
Stiffness coefficient of seat k_s	17830 N/m
Stiffness coefficient of torso k_1	49340 N/m
Damping coefficient of seat c_s	1500 Ns/m
Damping coefficient of torso c_1	2475 Ns/m

Table 2. Parameters of MR damper (Phu et al., 2020)

Parameter	Value
Stiffness of gas chamber k_e	94.6166 N/m
Damping coefficient c_e	794.4681 Ns/m
Piston area A_p	0.00113354 m^2
Piston rod area A_r	0.0000785 m^2
Gap of magnetic pole h	0.01 m
Length of magnetic pole L	0.05 m
MR inherent coefficient α_1	26.77185
MR inherent coefficient α_2	0.60444

Table 3. Parameters to calculate control current for MR damper (Phu et al., 2020)

Parameter	Value
Linear spring stiffness k_0	0 N/m
Viscous damping coefficient c_a	990 Ns/m
Viscous damping coefficient influenced by v c_b	3095 Ns/m V
Stiffness of φ_d α_a	545 N/m
Stiffness of φ_d influenced by v α_b	620 N/mV
Positive parameter of hysteresis loop φ	4
Positive parameter of hysteresis loop κ	48
Positive parameter of hysteresis loop λ	48

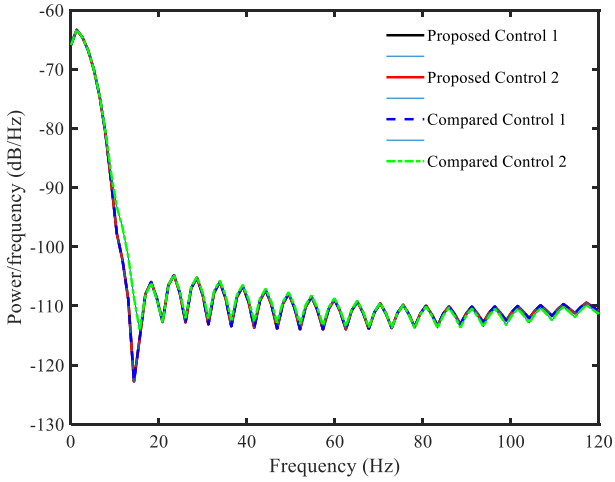

Fig. 3. Power spectral density index (PSD) of four controllers

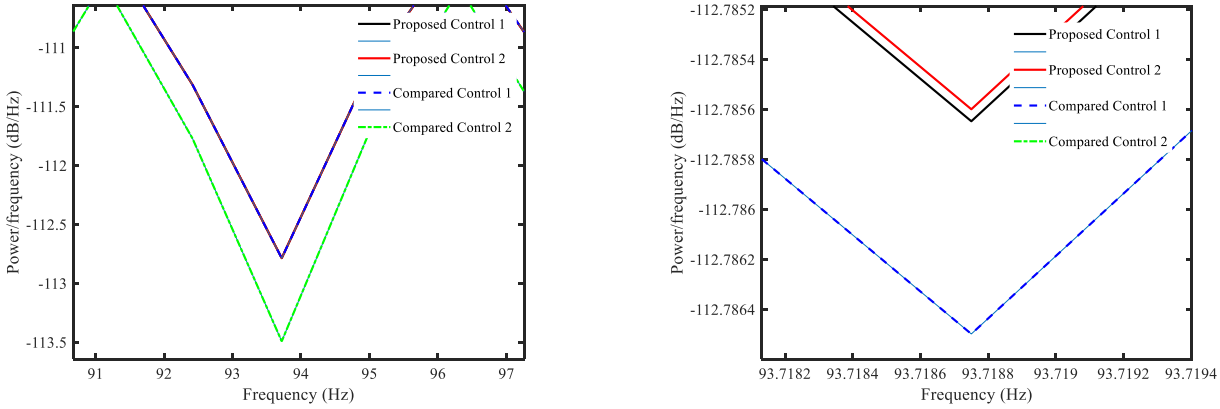

(a) Large scale 1 (b) Large scale 2

Fig. 4. Large scale of power spectral density (PSD) of four controllers

The simulation results are depicted in Figs. 3–9. Figs. 3 and 4 present a general view of the four compared controllers, displaying the power spectral density of the displacement. All four controllers demonstrate efficiency in controlling the severe disturbance, as shown in Fig. 3. However, the proposed controller 1 (Theorem 2.1) and proposed controller 2 (Theorem 2.2)

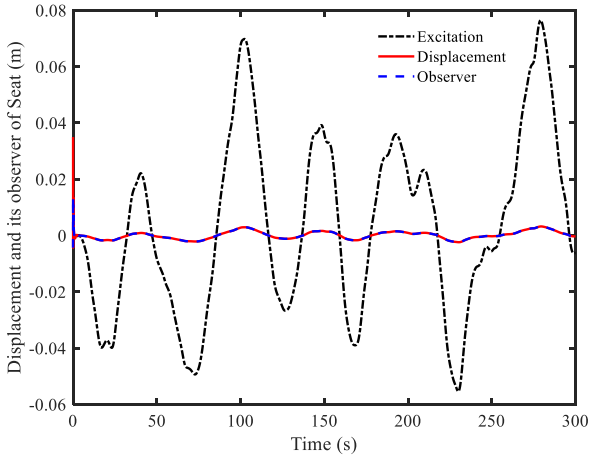

Fig. 5. Displacement response of the proposed controller 2

outperform the compared controllers, as shown in Fig. 4(a). Fig. 4(b) provides a clearer view of the proposed controller 1 and proposed controller 2, demonstrating that proposed controller 2 performs better than the other controllers. The reduction of the vibration amplitude achieved by proposed controller 2 can be observed in Fig. 5. It is noted that the large reduction in Fig. 5 is only obtained in simulation because of the properties of software with a fixed model of disturbance or data. This result may differ when applied in real applications with continuous disturbances from the unmodeled vibration of the machine. In the following analysis, the gain responses are reviewed. It is noteworthy that the adaptive gain function model is designed in proposed controller 1, proposed controller 2, and compared controller 1. The adaptive gain value in proposed controller 2 is stable and nearly zero, as shown in Fig. 6(b). This result differs from the adaptive gain of proposed controller 1 in Fig. 6(a) and compared controller 1 in Fig. 7. It is also important to point out that proposed controller 2 is the outstanding model for compensating the severe disturbance. After analyzing the gain values, the input control signals representing the power consumption of the four controllers are shown in Figs. 8 and 9. In these figures, the input force control of proposed controller 2 is stable and optimized, which is better than the other controllers. It is worth noting that the fluctuation in the input force control of proposed

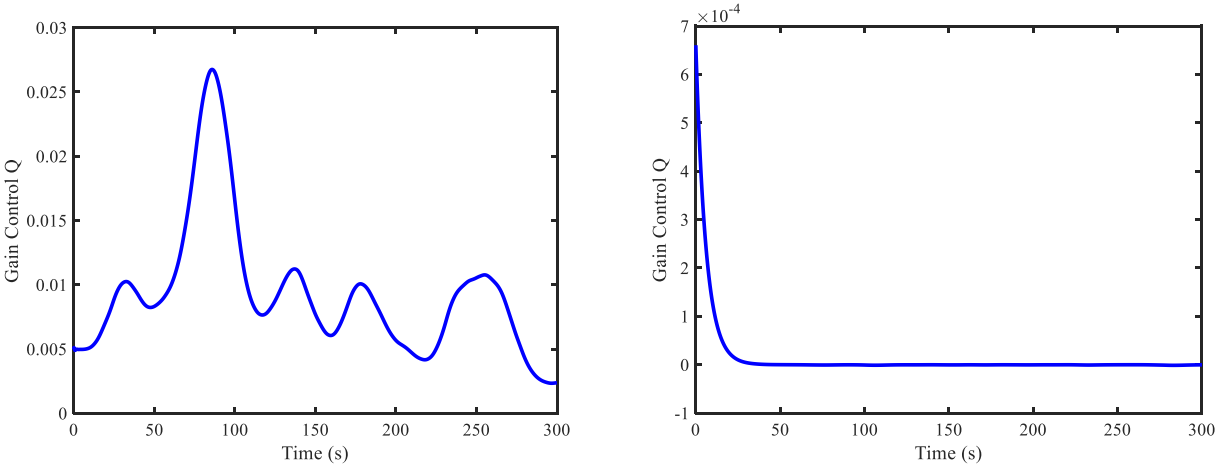

(a) Proposed controller 1 (b) Proposed controller 2

Fig. 6. Gain response

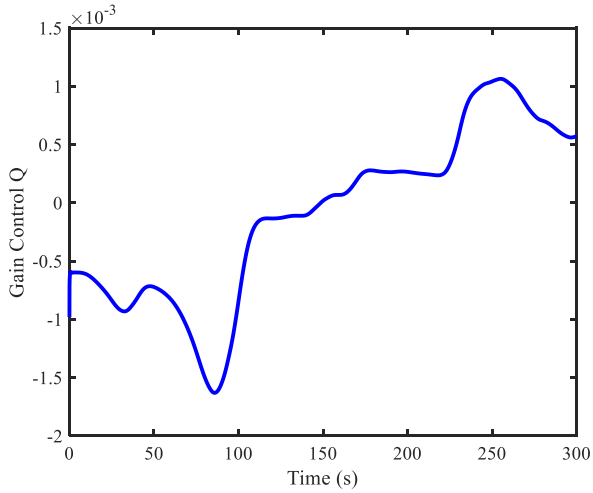

Fig. 7. Gain response of the compared controller 1 (Phu et al., 2020)

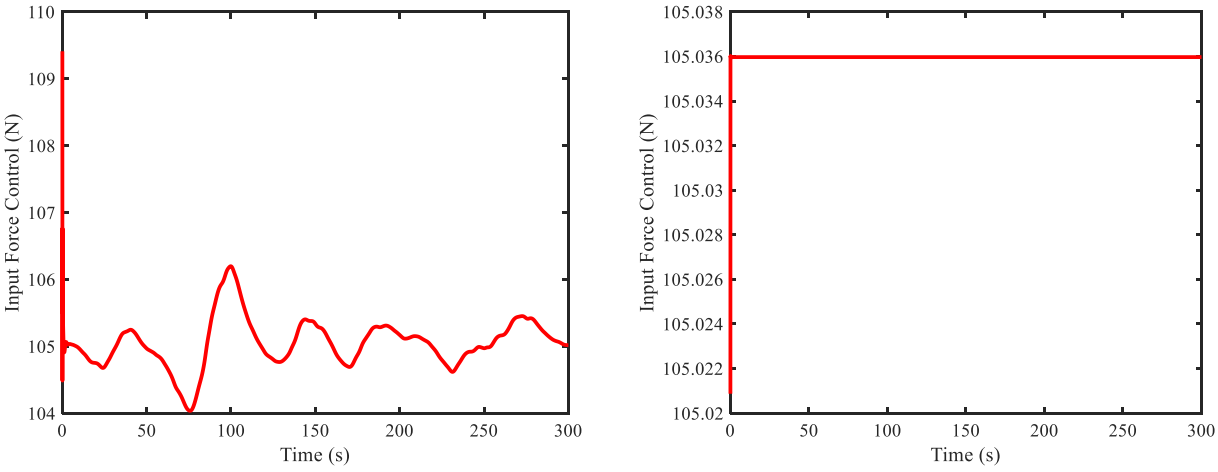

(a) Proposed controller 1 (b) Proposed controller 2

Fig. 8. Main input control

model 1 is also better than compared control 1, as shown in Figs. 8(a) and 9(a). Although the input force control of compared control 2 is stable, and its energy consumption is less than that of the other controls, its performance is not as good as shown in Fig. 4. It is clearly seen that the control forces of the proposed controllers 1 and 2 applied to the suspension system to suppress unwanted vibration are lower than those of the two compared controllers. This result directly indicates the lower power consumption to operate the vehicle seat suspension with MR damper. Generally, the proposed controls and the comparison controls demonstrate good performance under severe disturbances and uncertainties. The proposed control has significantly improved the operation through the PSD index by 84.442%, compared with 83.696% for the compared controls, as shown in Figs. 3 and 4. From the above results through the simulation with severe disturbance at the input data, the proposed control also shows potential for application in real systems, especially in devices with high amplitudes of vibration, and uncertainties. In addition, the proposed control can be applied in the case of cyber-attack phenomena to stabilize the operation of the system with the flexible mechanism in the state changes.

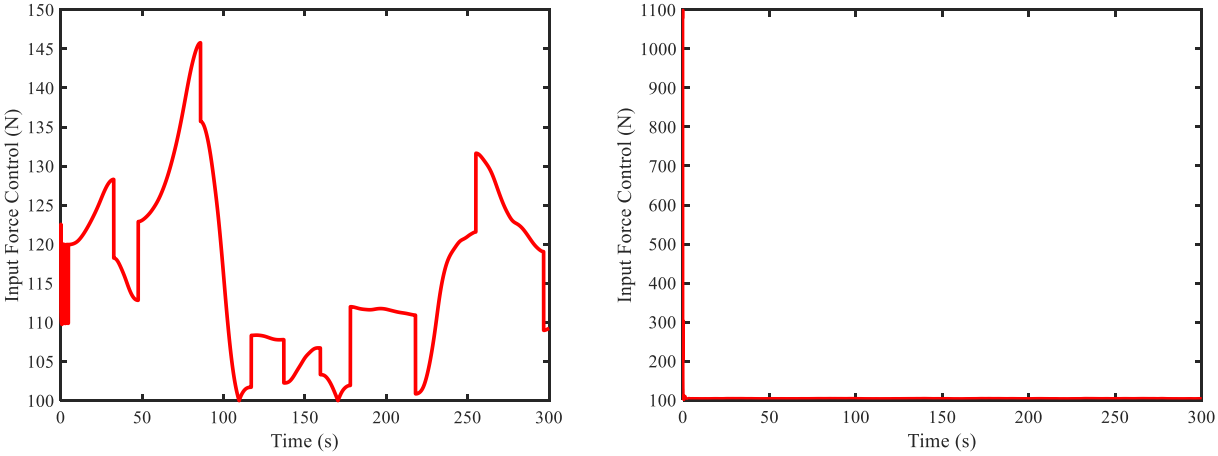

(a) Compared controller 1 (Phu et al., 2020) (b) Compared controller 2 (Kikuuwe et al., 2022)

Fig. 9. Main input control

4. CONCLUSION

In this study, two new models of the optimal control method based on two newly suggested adaptive gains are proposed and their performances are presented. The modified saturation functions are designed and applied to the proposed controllers. These proposed saturation functions are used to replace the conventional signum function in the control input to improve the system performance in response to severe disturbance and non-smooth vibration. In the first model, the saturation function with its differentiable property is described. A suggested modification in the denominator of the first model allows the saturation function to be differentiable with respect to time, while maintaining the conventional properties. In the second model, a new saturation-like function using the exponential signum function is applied. This model is divided into two cases depending on the boundary of the displacement. The applied cases are considered for controlling the non-smooth vibration or for operation under severe disturbance. The proposed models overcome the disadvantage of the conventional saturation function and open new perspectives in the design of adaptive optimal control laws with adaptive gain functions. After mathematically proving the stability of the system under the proposed controllers, the simulation of the proposed controllers is carried out. In the simulation, an automobile suspension with non-smooth vibration is used for evaluating the proposed controllers (Theorems 2.1 and 2.2). In addition, the simulation results are compared with the two existing controllers (Kikuuwe et al., 2022; Phu et al., 2020). Both the proposed controllers show their good performance in the non-smooth environment. It is clearly demonstrated that the second proposed controller (Theorem 2.2) outperforms the first proposed controller (in non-smooth vibration). These simulation results could serve as a basis for designing better optimal controllers that can adapt well to the properties and operating environments of the control systems. The results provide a foundation for application in real systems to overcome the limitations caused by disturbances, and save energy in control.

DECLARATION OF COMPETING INTEREST

The authors declare that they have no known competing financial interests or personal relationships that could have appeared to influence the work reported in this paper.

CREDIT AUTHOR STATEMENT

Xuan Phu Do: *Conceptualization, Methodology, Formal analysis, Investigation, Software, Data curation, Writing – original draft, Writing – review & editing, Visualization*.

ACKNOWLEDGEMENT

This research is funded by the Ministry of Education and Training Vietnam (MOET) under Grant number B2024-VGU-02.

REFERENCES

Basin, M., Loukianov, A. G., & Hernández-Fabián, R. (2011). An optimal sliding mode-like regulator for nonlinear polynomial systems. *International Journal of Systems Science*, *42*(11), 1909–1916. https://doi.org/10.1080/00207721.2010.545491

Basin, M., Rodriguez-Ramirez, P., Ferrara, A., & Calderon-Alvarez, D. (2012). Sliding mode optimal control for linear systems. *Journal of the Franklin Institute*, *349*(4), 1350–1363. https://doi.org/10.1016/j.jfranklin.2011.05.010

Deng, L., & Shen, J. (2021). Hurwicz model of uncertain linear quadratic optimal control with jump. *International Journal of Control*, *94*(6), 1455–1460. https://doi.org/10.1080/00207179.2019.1652768

Karg, P., Kopf, F., Braun, C. A., & Hohmann, S. (2023). Excitation for adaptive optimal control of nonlinear systems in differential games. *IEEE Transactions on Automatic Control*, *68*(1), 596–603. https://doi.org/10.1109/TAC.2022.3145651

Kikuuwe, R., Yamamoto, Y., & Brogliato, B. (2022). Implicit implementation of nonsmooth controllers to nonsmooth actuators. *IEEE Transactions on Automatic Control*, *67*(9), 4645–4657. https://doi.org/10.1109/TAC.2022.3163124

Li, Y., Liu, Y., & Tong, S. (2022). Observer-based neuro-adaptive optimized control of strict-feedback nonlinear systems with state constraints. *IEEE Transactions on Neural Networks and Learning Systems*, *33*(7), 3131–3145. https://doi.org/10.1109/TNNLS.2021.3051030

Li, Y., Wang, T., Liu, W., & Tong, S. (2022). Neural network adaptive output-feedback optimal control for active suspension systems. *IEEE Transactions on Systems, Man, and Cybernetics: Systems*, *52*(6), 4021–4032. https://doi.org/10.1109/TSMC.2021.3089768

Liu, M., Wan, Y., Lewis, F. L., & Lopez, V. G. (2020). Adaptive optimal control for stochastic multiplayer differential games using on-policy and off-policy reinforcement learning. *IEEE Transactions on Neural Networks and Learning Systems*, *31*(12), 5522–5533. https://doi.org/10.1109/TNNLS.2020.2969215

Liu, P., Hu, Q., Li, L., Liu, M., Chen, X., Piao, C., & Liu, X. (2022). Fast control parameterization optimal control with improved Polak–Ribière–Polyak conjugate gradient implementation for industrial dynamic processes. *ISA Transactions*, *123*, 188–199. https://doi.org/10.1016/j.isatra.2021.05.020

Modares, H., Lewis, F. L., & Naghibi-Sistani, M.-B. (2013). Adaptive optimal control of unknown constrained-input systems using policy iteration and neural networks. *IEEE Transactions on Neural Networks and Learning Systems*, *24*(10), 1513–1525. https://doi.org/10.1109/TNNLS.2013.2276571

Phu, D. X., Huy, T. D., Mien, V., & Choi, S.-B. (2018). A new composite adaptive controller featuring the neural network and prescribed sliding surface with application to vibration control. *Mechanical Systems and Signal Processing*, *107*, 409–428. https://doi.org/10.1016/j.ymssp.2018.01.040

Phu, D. X., & Mien, V. (2020). Robust control for vibration control systems with dead-zone band and time delay under severe disturbance using adaptive fuzzy neural network. *Journal of the Franklin Institute*, *357*(17), 12281–12307. https://doi.org/10.1016/j.jfranklin.2020.09.011

Phu, D. X., Mien, V., Thanh Tu, P. H., Nguyen, N. P., & Choi, S.-B. (2020). A new optimal sliding mode controller with adjustable gains based on Bolza-Meyer criterion for vibration control. *Journal of Sound and Vibration*, *485*, 115542. https://doi.org/10.1016/j.jsv.2020.115542

Phu Do, X., Hung Nguyen, Q., & Choi, S.-B. (2019). New hybrid optimal controller applied to a vibration control system subjected to severe disturbances. *Mechanical Systems and Signal Processing*, *124*, 408–423. https://doi.org/10.1016/j.ymssp.2019.01.036

Sai, H., Xu, Z., He, S., Zhang, E., & Zhu, L. (2022). Adaptive nonsingular fixed-time sliding mode control for uncertain robotic manipulators under actuator saturation. *ISA Transactions*, *123*, 46–60. https://doi.org/10.1016/j.isatra.2021.05.011

Soler, M., Kamgarpour, M., Lloret, J., & Lygeros, J. (2016). A hybrid optimal control approach to fuel-efficient aircraft conflict avoidance. *IEEE Transactions on Intelligent Transportation Systems*, *17*(7), 1826–1838. https://doi.org/10.1109/TITS.2015.2510824

Song, R., Lewis, F. L., Wei, Q., & Zhang, H. (2016). Off-policy actor-critic structure for optimal control of unknown systems with disturbances. *IEEE Transactions on Cybernetics*, *46*(5), 1041–1050. https://doi.org/10.1109/TCYB.2015.2421338

Sui, S., Li, Y., & Tong, S. (2016). Observer-based adaptive fuzzy control for switched stochastic nonlinear systems with partial tracking errors constrained. *IEEE Transactions on Systems, Man, and Cybernetics: Systems*, *46*(12), 1605–1617. https://doi.org/10.1109/TSMC.2016.2523904

Tong, S., Sun, K., & Sui, S. (2018). Observer-based adaptive fuzzy decentralized optimal control design for strict-feedback nonlinear large-scale systems. *IEEE Transactions on Fuzzy Systems*, *26*(2), 569–584. https://doi.org/10.1109/TFUZZ.2017.2686373

Vamvoudakis, K. G., Miranda, M. F., & Hespanha, J. P. (2016). Asymptotically stable adaptive–optimal control algorithm with saturating actuators and relaxed persistence of excitation. *IEEE Transactions on Neural Networks and Learning Systems*, *27*(11), 2386–2398. https://doi.org/10.1109/TNNLS.2015.2487972

Xiao, W., Belta, C. A., & Cassandras, C. G. (2022). Sufficient conditions for feasibility of optimal control problems using Control Barrier Functions. *Automatica*, *135*, 109960. https://doi.org/10.1016/j.automatica.2021.109960

Zhang, Y., Li, S., & Liu, X. (2018). Adaptive near-optimal control of uncertain systems with application to underactuated surface vessels. *IEEE Transactions on Control Systems Technology*, *26*(4), 1204–1218. https://doi.org/10.1109/TCST.2017.2705057

APPENDIX A. DERIVATION OF EQ. (8)

Consider the optimal control problem for the system (1) with respect to the Bolza criterion without a non-integral term

$$J = \frac{1}{2}\int_{to}^{T} \left(u_{\nabla}^{T}(s)\, R_{\nabla}(s)\, u_{\nabla}(s) + x_{\nabla}^{T}(s)\, L_{\nabla}(s)\, x_{\nabla}(s) \right) \mathrm{d}s. \tag{A.1}$$

In this analysis, Eq. (4) is simplified as $q_{\nabla}(t) = \alpha Q_{\nabla}(t)\, x_{\nabla}(t)$. The optimal control law is found as follows

$$u_{\nabla}^{*}(t) = -R_{\nabla}^{-1}(t)\, B_{\nabla}{}^{T}(t)\, (\alpha Q_{\nabla}(t)\, x_{\nabla}(t)) = -\alpha R_{\nabla}^{-1}(t)\, B_{\nabla}^{T}(t)\, Q_{\nabla}(t)\, x_{\nabla}(t), \tag{A.2}$$

where, the gain matrix $Q_\nabla(t)$ is found from $\frac{\mathrm{d}q_\nabla}{\mathrm{d}t} = -\frac{\partial H}{\partial x_\nabla}$, and the Hamilton function $H(x_\nabla, u_\nabla, q_\nabla, t) = \frac{1}{2}\left(u_\nabla^T R_\nabla(t) u_\nabla + x_\nabla^T L_\nabla(t) x_\nabla\right) + q_\nabla^T \dot{x}_\nabla(t)$ as follows

$$\begin{aligned}
&\alpha\dot{Q}_\nabla(t) x_\nabla(t) + \alpha Q_\nabla(t)\dot{x}_\nabla(t) = -L_\nabla(t) x_\nabla(t) - \left[\frac{\partial f_\nabla(x_\nabla, t)}{\partial x_\nabla}\right]^T (\alpha Q_\nabla(t) x_\nabla(t)) \\
&\Leftrightarrow \alpha\dot{Q}_\nabla x_\nabla(t) = -L_\nabla(t) x_\nabla(t) - [a_{1\nabla}(t) + 2a_{2\nabla}(t)x_\nabla(t) + 3a_{3\nabla}(t)x_\nabla(t)x_\nabla^T(t) \\
&\quad + ... + pa_{p\nabla}(t)x_\nabla(t)...{}_{p-1\ times}...x_\nabla(t)]^T (\alpha Q_\nabla(t)x_\nabla(t)) \\
&\quad - \alpha Q_\nabla(t)[a_{0\nabla}(t) + a_{1\nabla}(t)x_\nabla(t) + a_{2\nabla}(t)x_\nabla(t)x_\nabla^T(t) + ... + a_{p\nabla}(t)x_\nabla(t)...{}_{p-1\ times}\ldots x_\nabla(t)] \\
&\quad + \alpha^2 Q_\nabla(t)B_\nabla(t){R_\nabla}^{-1}(t){B_\nabla}^T(t)Q_\nabla(t)x_\nabla(t) \\
&\Leftrightarrow \dot{Q}_\nabla(t) = -\frac{1}{\alpha}L_\nabla(t) - [a_{1\nabla}(t) + 2a_{2\nabla}(t)x_\nabla(t) + 3a_{3\nabla}(t)x_\nabla(t)x_\nabla^T(t) \\
&\quad + ... + pa_{p\nabla}(t)x_\nabla(t)...{}_{p-1\ times}...x_\nabla(t)]^T Q_\nabla(t) - Q_\nabla(t)a_{0\nabla}(t){x_\nabla}^{-1}(t) \\
&\quad - Q_\nabla(t)[a_{1\nabla}(t) + a_{2\nabla}(t)x(t) + a_{3\nabla}(t)x_\nabla(t)x_\nabla^T + \cdots + a_{p\nabla}(t)x_\nabla(t)\ldots{}_{p-1\ times,}\ldots x_\nabla(t)] \\
&\quad + \alpha Q_\nabla(t)B_\nabla(t){R_\nabla}^{-1}(t){B_\nabla}^T(t)Q_\nabla(t).
\end{aligned} \tag{A.3}$$

From Eq. (A.2), the new gain matrix $\alpha Q_\nabla(t) x_\nabla(t)$ can be rewritten by $Q_{\Delta\Delta} = \alpha Q_\nabla(t)|x_\nabla(t)|$. The derivative of the new modified gain matrix is derived as follows

$$\begin{aligned}
\dot{Q}_{\Delta\Delta}(t) &= \frac{\mathrm{d}(\alpha Q_\nabla(t)x_\nabla^2(t))}{\mathrm{d}t} = \alpha\frac{\mathrm{d}Q_\nabla(t)}{\mathrm{d}t}|x_\nabla(t)| + \alpha Q_\nabla(t)\frac{\mathrm{d}(|x_\nabla(t)|)}{\mathrm{d}t} \\
&= -L_\nabla(t)|x_\nabla(t)| - \alpha([a_{1\nabla}(t) + 2a_{2\nabla}(t)x_\nabla(t) + 3a_{3\nabla}(t)x_\nabla(t)x_\nabla^T + ... \\
&\quad + pa_{p\nabla}(t)x_\nabla(t)...{}_{p-1\ times,}\ldots x_\nabla(t)]^T Q_\nabla(t))|x_\nabla(t)| - \alpha Q_\nabla(t)a_{0\nabla}(t) \\
&\quad - \alpha(Q_\nabla(t)[a_{1\nabla}(t) + a_{2\nabla}(t)x_\nabla(t) + a_{3\nabla}(t)x_\nabla(t)x_\nabla^T + \cdots \\
&\quad + a_{p\nabla}(t)x_\nabla(t)\ldots{}_{p-1\ times,}\ldots x_\nabla(t)]|x_\nabla(t)| \\
&\quad + \alpha^2 Q_\nabla(t)B_\nabla(t){R_\nabla}^{-1}(t){B_\nabla}^T(t)Q_\nabla(t))|x_\nabla(t)| \\
&\quad + \alpha Q_\nabla(t)a_{0\nabla}(t) + \alpha Q_\nabla(t)[a_{1\nabla}(t) + a_{2\nabla}(t)x_\nabla(t) + a_{3\nabla}(t)x_\nabla(t)x_\nabla^T + \cdots \\
&\quad + a_{p\nabla}(t)x_\nabla(t)\ldots{}_{p-1\ times,}\ldots x_\nabla(t)]|x_\nabla(t)| - \alpha R_\nabla^{-1}(t){B_\nabla}^T(t)Q_\nabla(t)|x_\nabla(t)|) \\
&= -L_\nabla(t)|x_\nabla(t)| - \alpha[a_{1\nabla}(t) + 2a_{2\nabla}(t)x_\nabla(t) + 3a_{3\nabla}(t)x_\nabla(t)x_\nabla^T + ... \\
&\quad + pa_{p\nabla}(t)x_\nabla(t)\ldots{}_{p-1\ times,}\ldots x_\nabla(t)]^T Q_\nabla(t))|x_\nabla(t)|.
\end{aligned} \tag{A.4}$$

APPENDIX B. DERIVATION OF EQ. (25)

Consider the optimal control problem for the system (1) with respect to the Bolza criterion without a non-integral term

$$J_e = \frac{1}{2}\int_{to}^{T}\left(u_{e\nabla}^T(s) R_{e\nabla}(s) u_{e\nabla}(s) + x_{e\nabla}^T(s) L_{e\nabla}(s) x_{e\nabla}(s)\right)\mathrm{d}s. \tag{B.1}$$

Using Eq. (21), the optimal control law is found as follows

$$\begin{aligned}
u_{e\nabla}^*(t) &= -R_{e\nabla}^{-1}(t) {B_{e\nabla}}^T(t) q_{e\nabla}(t) \\
&= \begin{cases} -\alpha_e R_{e\nabla}^{-1}{B_{e\nabla}}^T Q_{e\nabla}\left(k_1 sig^r(x_{e\nabla}) + k_2\delta^{|x_{e\nabla}|}x_{e\nabla}\right) & \text{if } |x_{e\nabla}| < \delta, \\ -\alpha_e R_{e\nabla}^{-1}{B_{e\nabla}}^T Q_{e\nabla} sig^\beta(x_{e\nabla}) & \text{if } |x_{e\nabla}| > \delta, \end{cases}
\end{aligned} \tag{B.2}$$

where the gain matrix $Q_{e\nabla}(t)$ is found from $\frac{\mathrm{d}q_{e\nabla}}{\mathrm{d}t} = -\frac{\partial H}{\partial x_{e\nabla}}$, and the Hamilton function $H(x_{e\nabla}, u_{e\nabla}, q_{e\nabla}, t) = \frac{1}{2}\left(u_{e\nabla}^T R_{e\nabla}(t) u_{e\nabla} + x_{e\nabla}^T L_{e\nabla}(t) x_{e\nabla}\right) + q_{e\nabla}^T \dot{x}_{e\nabla}(t)$ as follows:

Case 1. $|x_{e\nabla}| < \delta$

Using Eqs. (21), (30), (31), the following equation is obtained

$$\begin{aligned}
&-\alpha_e \dot{Q}_{e\nabla}\left(k_1 sig^r(x_{e\nabla}) + k_2\delta^{|x_{e\nabla}|}x_{e\nabla}\right) - \alpha_e Q_{e\nabla}\frac{\mathrm{d}\left(k_1 sig^r(x_{e\nabla}) + k_2\delta^{|x_{e\nabla}|}x_{e\nabla}\right)}{\mathrm{d}t} \\
&= L_{e\nabla}x_{e\nabla} + \alpha_e\begin{bmatrix} a_{1e\nabla} + 2a_{2e\nabla}x_{e\nabla} + 3a_{3e\nabla}x_{e\nabla}x_{e\nabla}^T + \ldots \\ + pa_{pe\nabla}x_{e\nabla}\cdots_{(p-1)times}\ldots x_{e\nabla}\end{bmatrix}^T Q_{e\nabla}\left(k_1 sig^r(x_{e\nabla}) + k_2\delta^{|x_{e\nabla}|}x_{e\nabla}\right) \\
&\Leftrightarrow -\alpha_e \dot{Q}_{e\nabla}\left(k_1 sig^r(x_{e\nabla}) + k_2\delta^{|x_{e\nabla}|}x_{e\nabla}\right) - \alpha_e Q_{e\nabla}\left(k_1 r|x_{e\nabla}|^{r-1} + k_2\left(|x_{e\nabla}|\ln\delta + 1\right)\delta^{|x_{e\nabla}|}\right) \\
&= L_{e\nabla}x_{e\nabla} + \alpha_e\begin{bmatrix} a_{1e\nabla} + 2a_{2e\nabla}x_{e\nabla} + 3a_{3e\nabla}x_{e\nabla}x_{e\nabla}^T + \ldots \\ + pa_{pe\nabla}x_{e\nabla}\cdots_{(p-1)times}\ldots x_{e\nabla}\end{bmatrix}^T Q_{e\nabla}\left(k_1 sig^r(x_{e\nabla}) + k_2\delta^{|x_{e\nabla}|}x_{e\nabla}\right) \\
&\Leftrightarrow \dot{Q}_{e\nabla} = -\frac{1}{\alpha_e\left(k_1 sig^r(x_{e\nabla}) + k_2\delta^{|x_{e\nabla}|}x_{e\nabla}\right)}L_{e\nabla}x_{e\nabla} \\
&\quad -\begin{bmatrix} a_{1e\nabla} + 2a_{2e\nabla}x_{e\nabla} + 3a_{3e\nabla}x_{e\nabla}x_{e\nabla}^T + \ldots + \\ + pa_{pe\nabla}x_{e\nabla}\cdots_{(p-1)times}\ldots x_{e\nabla}\end{bmatrix}^T Q_{e\nabla} \\
&\quad - Q_{e\nabla}\frac{\left(k_1 r|x_{e\nabla}|^{r-1} + k_2\left(|x_{e\nabla}|\ln\delta + 1\right)\delta^{|x_{e\nabla}|}\right)}{\left(k_1 sig^r(x_{e\nabla}) + k_2\delta^{|x_{e\nabla}|}x_{e\nabla}\right)}.
\end{aligned} \tag{B.3}$$

The result (B.3) can be analyzed following inequality method as follows

$$\begin{aligned}
\Leftrightarrow \dot{Q}_{e\nabla} &\le -\alpha_e L_{e\nabla}|x_{e\nabla}| - a_{1e\nabla}Q_{e\nabla} + \alpha_e Q_{e\nabla}k_1 r|x_{e\nabla}|^{r-1} \\
&\le -\alpha_e L_{e\nabla}x_{e\nabla}^2 - \nu a_{1e\nabla}Q_{e\nabla} + \alpha_e \nu Q_{e\nabla}k_1 r x_{e\nabla}^2.
\end{aligned} \tag{B.4}$$

From Eq. (B.4), the new gain matrix $Q_{e\nabla}(t)$ can be found following the derivative of the new modified gain matrix as follows

$$\dot{Q}_{e\nabla} = -\alpha_e L_{e\nabla}x_{e\nabla}^2 - \nu\left(a_{1e\nabla} + \alpha_e k_1 r x_{e\nabla}^2\right)Q_{e\nabla}. \tag{B.5}$$

Case 2. $|x_{e\nabla}| > \delta$

Using Eqs. (21), (30), (31), the following equation is obtained

$$\begin{aligned}
&-\alpha_e \dot{Q}_{e\nabla} sig^\beta(x_{e\nabla}) - \alpha_e Q_{e\nabla}\frac{\mathrm{d}\left(sig^\beta(x_{e\nabla})\right)}{\mathrm{d}t} = L_{e\nabla}x_{e\nabla} \\
&+\alpha_e\begin{bmatrix} a_{1e\nabla} + 2a_{2e\nabla}x_{e\nabla} + 3a_{3e\nabla}x_{e\nabla}x_{e\nabla}^T + \ldots \\ + pa_{pe\nabla}x_{e\nabla}\cdots_{(p-1)times}\ldots x_{e\nabla}\end{bmatrix}^T Q_{e\nabla} sig^\beta(x_{e\nabla}) \\
\Leftrightarrow \dot{Q}_{e\nabla} &= -\frac{1}{\alpha_e sig^\beta(x_{e\nabla})}L_{e\nabla}x_{e\nabla} \\
&\quad -\begin{bmatrix} a_{1e\nabla} + 2a_{2e\nabla}x_{e\nabla} + 3a_{3e\nabla}x_{e\nabla}x_{e\nabla}^T + \ldots \\ + pa_{pe\nabla}x_{e\nabla}\cdots_{(p-1)times}\ldots x_{e\nabla}\end{bmatrix}^T Q_{e\nabla} - \frac{1}{sig^\beta(x_{e\nabla})}\beta Q_{e\nabla}|x_{e\nabla}|^{\beta-1}.
\end{aligned} \tag{B.6}$$

The result (B.6) can be analyzed following inequality method as follows

$$\begin{aligned}
&\Leftrightarrow -\alpha_e \dot{Q}_{e\nabla} sig^{\beta}\left(x_{e\nabla}\right) - \alpha_e \beta Q_{e\nabla} |x_{e\nabla}|^{\beta-1} = L_{e\nabla} x_{e\nabla} \\
&\quad + \alpha_e \begin{bmatrix} a_{1e\nabla} + 2a_{2e\nabla} x_{e\nabla} + 3a_{3e\nabla} x_{e\nabla} x_{e\nabla}^T + ... \\ + p a_{pe\nabla} x_{e\nabla} \cdots_{(p-1)times} \cdots x_{e\nabla} \end{bmatrix}^T Q_{e\nabla} sig^{\beta}\left(x_{e\nabla}\right) \\
&\Leftrightarrow \dot{Q}_{e\nabla} \leq -\alpha_e L_{e\nabla} |x_{e\nabla}| - a_{1e\nabla} Q_{e\nabla} + \alpha_e Q_{e\nabla} \beta |x_{e\nabla}|^{\beta-1} \\
&\qquad \leq -\alpha_e L_{e\nabla} x_{e\nabla}^2 - \nu a_{1e\nabla} Q_{e\nabla} + \alpha_e \nu Q_{e\nabla} \beta x_{e\nabla}^2.
\end{aligned} \tag{B.7}$$

From Eq. (B.7), the new gain matrix $Q_{e\nabla}(t)$ can be found following the derivative of the new modified gain matrix as follows

$$\dot{Q}_{e\nabla} = -\alpha_e L_{e\nabla} x_{e\nabla}^2 - \nu \left(a_{1e\nabla} + \alpha_e \beta x_{e\nabla}^2\right) Q_{e\nabla}. \tag{B.8}$$